Probing the "Dark" Fraction of Core–Shell Quantum Dots by Ensemble and Single Particle pH-Dependent Spectroscopy

Nela Durisic,[†] Antoine G. Godin,[†] Derrel Walters,[‡] Peter Grütter,[†,*] Paul W. Wiseman,[†,§,*] and Colin D. Heyes[‡,*]

[†]Department of Physics, McGill University, 3600 Rue University, Montreal, Quebec, Canada H3A 2T8, [‡]Department of Chemistry and Biochemistry, University of Arkansas, 345 North Campus Drive, Fayetteville, Arkansas 72701, United States, and [§]Department of Chemistry, McGill University, 800 Rue Sherbrooke Ouest, Montreal, Quebec, Canada H3A 2K6

ABSTRACT

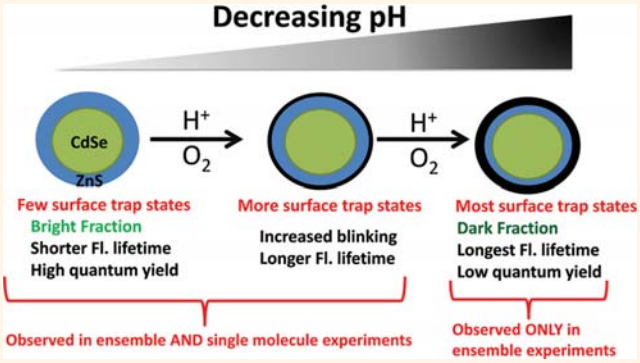

The optical properties of core–shell CdSe–ZnS quantum dots (QDs) are characterized by complex photophysics leading to difficulties in interpreting quantitative measurements based on QD emission. By comparing the pH dependence of fluorescence of single QDs to that of an ensemble, we have been able to propose a molecular scale model of how QD surface chemical and physical processes are affected by protons and oxygen. We show that the connection between the ensemble fluorescence intensity and the single QD fluorescence properties such as dark fraction, blinking, particle brightness, and a multiexponential fluorescence lifetime decay is not trivial. The ensemble fluorescence intensity is more weakly dependent on pH than the single particle fluorescence which, together with fluorescence lifetime analysis, provided evidence that the dark fraction of QDs emits photons with low quantum efficiency and long lifetime. We uncovered two surface-dependent mechanisms that affected the fluorescence emission: an immediate physical effect of charges surrounding the QD and an irreversible chemical effect from reaction of the H^+ and O_2 with the QD shell surface. These results will have important implications for those using QD-based fluorescence lifetime imaging as well as for proper implementation of these probes for quantitative cellular imaging applications.

KEYWORDS: dark fraction · core–shell quantum dots · fluorescence lifetime

The development of reproducible colloidal synthesis methods for quantum dots (QDs)[1–4] and their commercial availability from a number of sources have opened up possibilities for their use in many electronic and photonic applications. Arguably, the most developed application for QDs based on CdSe and CdTe is their use as fluorescent tags for biomolecules.[5–10] Despite their promise for photonics applications, the optical properties of QDs are characterized by complicated photophysics including irreproducible and unpredictable quantum yields, intermittent on/off switching of the fluorescence emission (blinking), non-exponential fluorescence lifetime decays, and the existence of a dark fraction within QD samples, leading to challenges in extracting *quantitative* information based on QD emission. While intrinsic exciton dynamics of QDs are generally understood,[11,12] the influence of extrinsic factors, such as the solution environment, is less so due to a lack of understanding at the microscopic level of the physical and chemical basis for the observations.

The quantum yield of a single CdSe QD has been shown to be significantly different from the ensemble quantum yield,[13,14] and the difference has been attributed largely to the presence of a dark fraction of non-emitting nanoparticles in the sample.[13,15] This dark fraction has been shown to be highly dependent on sample quality and experimental conditions, such as pH.[14,16,17] Nonradiative relaxation pathways may be enhanced by the presence of energetically deep or shallow surface trap states.[18,19] Shallow trap emission is generally energetically indistinguishable from band edge emission but has a longer fluorescence lifetime.[20,21] Therefore, fluorescence lifetime curves monitored at the band edge are generally multiexponential due to the contribution from these surface states. Deep traps are much lower in energy (red-shifted by more than 100 nm), energetically broad, weak in intensity, and have lifetimes at least an order of magnitude longer than the tens of nanoseconds characteristic of shallow trap emission.[22,23] Systematic studies of the fluorescence lifetimes of QDs under various conditions offer valuable insight into the effects of these variables on

* Address correspondence to cheyes@uark.edu, paul.wiseman@mcgill.ca, peter.grutter@mcgill.ca.

Received for review August 24, 2011 and accepted October 24, 2011.

Published online October 24, 2011
10.1021/nn203272p

the range of photophysical processes that characterize these nanoparticles.[18,24] Modification of a number of external environmental factors that influence the optical properties of QDs, such as the addition of electron donors and/or acceptors to the solution, has been shown to affect fluorescence quenching,[17,25−28] blinking,[17,29−31] dark fraction,[17] and fluorescence lifetime.[31,32] Recent reports have shown that environmental factors can affect both the radiative and nonradiative rates simultaneously and unpredictably,[31] which further complicates the interpretation. Additionally, the shell thickness and chemical composition of core−shell QDs have been shown to be important parameters that affect the optical properties.[33−36]

Connecting the observed single particle optical properties of QDs to the macroscopic optical response of a quantum dot ensemble, under a variety of conditions, is necessary for improving our understanding of the physical basis of the observed macroscopic properties. It is important to consider the wide range of variables that affect optical properties when comparing data from various samples and to control these variations by performing all measurements on the same sample of QDs. In this study, we systematically probe various fluorescence properties of CdSe−ZnS core−shell QDs with both single particle and ensemble level measurements as a function of solution pH in the range between 6 and 9. We chose to perform a pH-dependent study since the effects of pH on the ensemble fluorescence properties for a number of QD preparations have been reported by different groups,[37−42] and recent applications of QDs as pH sensors have been proposed.[43,44] Moreover, pH is a key parameter in biological studies and varies in different subcellular compartments. For quantitative fluorescence microscopy applications, the concentration of QDs (and therefore QD-labeled biomolecules) in cells is often estimated using their fluorescence intensity and ensemble quantum yield. However, a change in the dark fraction, blinking, and quantum yield (resulting from changes in radiative and nonradiative rates) can result in the erroneous determination of concentration−intensity relationships, which in turn limits the quantitative conclusions drawn from such studies. There have been recent reports of using pH-induced fluorescence intensity changes of QDs to monitor biological systems at the subcellular level.[45,46] Such studies highlight the need to thoroughly understand the physical and chemical basis for the pH effects on QD optical properties.

Using CdSe−ZnS core−shell QDs, we found that pH strongly and irreversibly affects both the intensity and fluorescence lifetime at the QD ensemble level, which vary as a function of time of exposure to the different pH solutions. By relating the pH dependence of the ensemble fluorescence intensity and lifetime to that of the single particle fluorescence lifetime, blinking, and dark fraction formation for the same QD samples,[17] we propose a mechanistic model of how both chemical and physical processes are affected by pH and influence the observed optical properties.

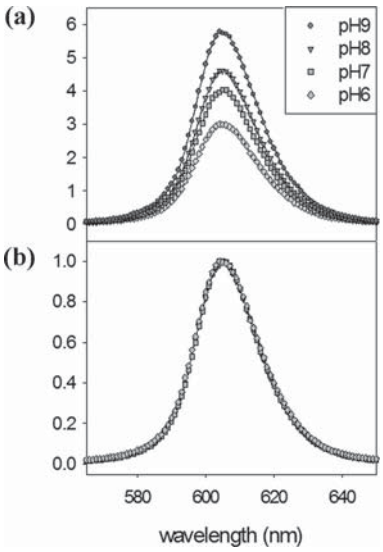

Figure 1. Effect of pH on the QD emission spectrum. (a) Fluorescence intensity decreases with pH, but (b) the normalized spectra show the peak position does not change, which indicates that the core size stays the same. Spectra are measured with 1 nm resolution.

RESULTS

pH Irreversibly Affects the Ensemble Fluorescence Intensity but Not the Emission Spectrum. Figure 1a shows the fluorescence emission spectra of QDs in solutions with pH values ranging from 6 to 9, while Figure 1b shows the same data, normalized, to highlight the fact that, while the fluorescence intensity decreased as the pH was lowered, there was no shift in the emission peak wavelength over this pH range, highlighting that the effects are not due to changes in QD size.

As the QDs were exposed to the pH-adjusted salt solutions, the fluorescence intensity decreased as a function of time. Figure 2a shows the relative decrease in the mean intensity of the emission peak, normalized at $t = 0$, measured as a function of time of exposure of the QD ensemble to PBS solutions of different pH. The fluorescence emission decayed faster as the pH decreased. After about 30 min, a plateau was reached, with the fluorescence reduced by 34% of its initial value at pH 9 and by 88% at pH 6. We determined that the salt ions present in the PBS solutions did not act as fluorescence quenching agents by measuring the fluorescence as a function of potassium phosphate and sodium chloride concentrations and did not observe any change in the emission intensity on these time scales (Supporting Information). We also determined that the absorption spectrum of the QDs in pH 6 solution was the same at $t = 0$ and $t = 6000$ s to ensure that no changes in the QD size occurred as a function of exposure time (Supporting Information).

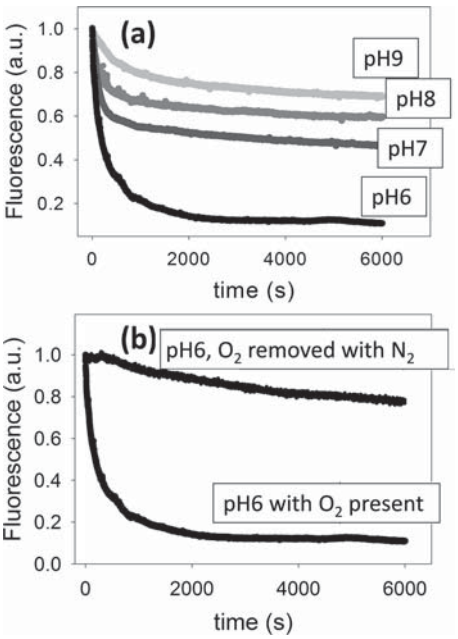

Figure 2. (a) Ensemble fluorescence intensity of QDs as a function of time exposed to different pH solutions. (b) Effect of oxygen removal on ensemble fluorescence intensity decay of QDs exposed to pH 6, indicating that both oxygen and H^+ are important. The fluorescence intensity was measured at 605 nm with 1 s time resolution.

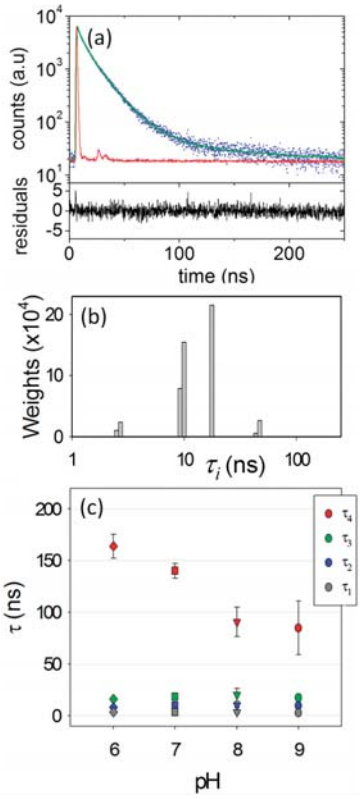

Figure 3. (a) Representative ensemble fluorescence intensity decay of QDs following excitation with pulsed light source with the best fit line to the data (green), instrument response function (red), and corresponding weighted residuals (black). The best fit line is obtained by recovering the amplitudes for a set of fixed lifetimes using a publically available MLE-based algorithm.[49] (b) Recovered amplitudes of lifetime constants (τ_i) from a single decay curve (as represented in panel a). Four lifetime decay components were recovered for the decay curves measured at each pH. (c) Effect of pH on each of the recovered lifetime decay components. It is important to highlight that the number of lifetime components was not fixed prior to fitting (see text), but the decay curves for each pH independently recovered four lifetime components. The error bars are the standard deviations of 30 consecutive measurements.

To investigate whether dissolved oxygen was involved in the fluorescence decay, we bubbled N_2 through the PBS solution in a sealed cuvette for 2 h to remove dissolved oxygen prior to introducing the QDs. Figure 2b compares the intensity decay with and without oxygen removal. In the pH 6 solution, the fluorescence intensity decays by only 25% over a period of 100 min, whereas it decayed by 88% with oxygen present, showing that oxygen plays a significant role in the pH-induced reduction of QD photostability. Sark *et al.* have previously shown that photooxidation of QDs in air leads to QD photobleaching.[47,48] However, in contrast to their observations, we do not observe a concomitant blue shift in the emission peak, suggesting that the core itself is unaffected by the pH and oxygen in solution. We also performed these pH stability experiments with QDs from another commercial source (Evident, Troy, NY) and found a similar trend. The exact time scale and extent of the decay varied, but the pH dependence was consistent, suggesting that the sample quality affects how quickly the fluorescence decays, but that it decays more rapidly for low pH solutions in the presence of oxygen. In general, chemical changes in the QD shell or at the core−shell interface could affect radiative and nonradiative recombination rates of photoinduced excitons without changing the emission energy.

pH Only Affects the Longest Fluorescence Lifetime Component of the QDs. Time-resolved information on exciton dynamics can be obtained from fluorescence lifetime measurements. Figure 3a shows a representative fluorescence decay curve for an ensemble of QDs together with multiexponential best fit curve from eq 7 and the resulting residuals. The multiexponential best fit curve is obtained by a publically available algorithm[49] based on a procedure described by Enderlein *et al.*[50] It is based on a maximum likelihood estimation (MLE) to determine the most probable lifetime components in the decay that have nonzero amplitude, described in more detail in the Experimental Section. The corresponding histogram of the recovered decay time and the number of photons detected from that process (weights) of a single decay curve is plotted in Figure 3b. This analysis was repeated for the decay curves at each pH, and for each of these curves, four distinct lifetimes were recovered and tabulated in Table 1. For the pH values sampled here, components $\tau_2 = 9 \pm 2$ ns and $\tau_3 = 18 \pm 3$ ns account for nearly 80% of the measured decay. The $\tau_1 = 3 \pm 1$ ns

TABLE 1. Fit Parameters and Standard Deviations of the Ensemble Lifetime Data Collected from QD Samples Exposed to PBS Solutions Whose pH Varied from 9 to 6 (Each Value Is an Average of 30 Consecutive Measurements)

	a_1 (%)	τ_1 (ns)	a_2 (%)	τ_2 (ns)	a_3 (%)	τ_3 (ns)	a_4 (%)	τ_4 (ns)
pH 9	9 ± 4	2.9 ± 0.6	46 ± 13	10 ± 2	43 ± 16	17 ± 3	7 ± 3	86 ± 33
pH 8	10 ± 4	3.5 ± 1.2	46 ± 17	10 ± 2	39 ± 20	20 ± 6	4 ± 1	91 ± 14
pH 7	8 ± 5	3.5 ± 1.5	42 ± 10	10 ± 1	43 ± 9	18 ± 1	6 ± 0.6	140 ± 7
pH 6	16 ± 9	3.4 ± 1.2	38 ± 10	8 ± 1	37 ± 10	16 ± 1	8 ± 1	164 ± 12

lifetime component is small in amplitude but remained constant within the fitting error, while τ_4 increased systematically when the pH was lowered.

Since the fluorescence intensity of the QDs decreased with time of exposure to the different pH solutions (Figure 2), we also determined how the fluorescence lifetime changes with time of exposure. Figure 2 indicates that most of the decay in emission signal occurred during the first 30 min of QD exposure to the pH-adjusted salt solutions; therefore, we measured the time-resolved decay kinetics every 60 s for 30 min at each pH value. As expected, each consecutive measurement in the time series exhibited a decrease in the total number of photon counts consistent with the ensemble results. Figure 4a shows that, for pH 9, only the slowest component τ_4 changes, increasing from 42.8 ± 6.2 ns, during the first 10 min, to 118.7 ± 23.9 ns in the last 10 min. At pH 6 (Figure 4b), τ_4 was initially measured to be 159 ± 7 ns during the first 10 min and slowly rose to 172 ± 10 ns in the last 10 min. The other three lifetime components were constant as a function of exposure time to all pH salt solutions and thus appeared to be pH-insensitive. Also, the amplitudes did not vary systematically with time of exposure but did show scatter (Figure 4c,d).

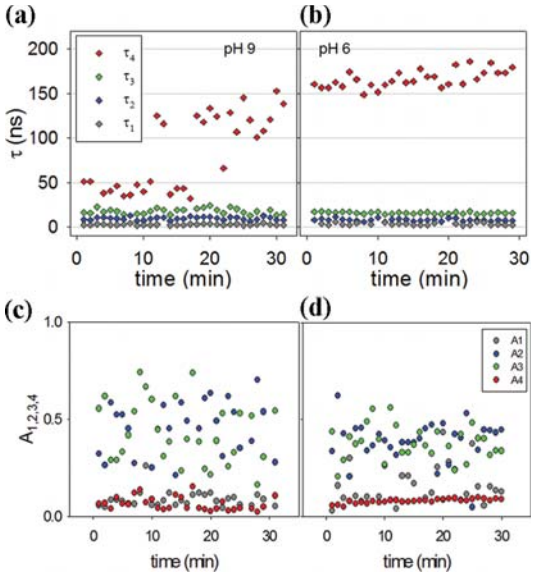

Figure 4. Changes in each of the recovered lifetime decay components (a,b) and their relative amplitudes (c,d) as a function of time of exposure to pH 9 and pH 6 solutions. A lifetime decay curve similar to panel (a) was measured every minute consecutively for 30 min.

Comparing the pH Dependence at the Ensemble Level and the Single Particle Level. Due to the differences in ensemble *versus* single molecule experimental detection, the photon flux of the excitation source needed to observe QDs at the single particle level is necessarily much higher than that used to observe ensemble QD signals. It is important to be wary of these differences when comparing results between ensemble and single QD experiments. However, provided the excitation conditions are held constant for all samples at each pH within a given experiment, the differences in pH *dependence* at the single particle and ensemble level should allow us to draw conclusions as to the molecular mechanism(s) that account(s) for the effect of H^+ ions in solution on the photophysical properties of the QDs.

Comparing pH Dependence of Fluorescence Intensity. Figure 5a shows images of resolved single QDs for different pH samples from which we extracted the pH dependence of the relative fraction of emitting QDs in a sample ("bright" fraction), the average fraction of emitting QDs that are "on" per 50 ms frame ("on" fraction), and the relative "on" intensity (single QD "brightness") (Figure 5b). The methods for extracting these parameters are described in detail in the Experimental Section. The pH dependence of the ensemble fluorescence intensity calculated from Figure 1a is also plotted in Figure 5b. The ensemble fluorescence intensity must be related to the single QD properties (dark fraction, blinking, and particle brightness), but the different pH dependencies of each property show that this relationship is not trivial. Between pH 9 and 8, the decrease in ensemble fluorescence intermittency coincides well with the decreasing "on" fraction of QDs, whereas the decrease in the "bright" fraction is much less pronounced. This suggests that increased blinking is primarily responsible for the decrease in the ensemble fluorescence intensity between pH 9 and 8. Our previous study on the blinking dynamics showed that the probability of observing long "on" times decreases and the probability of observing long "off" times increases between pH 9 to 6.[17] Once the pH was lowered below 8, both the "bright" fraction and the "on" fraction decreased more rapidly than the ensemble fluorescence intensity. These trends highlight the complexity of relating the single particle optical properties to the ensemble optical properties under

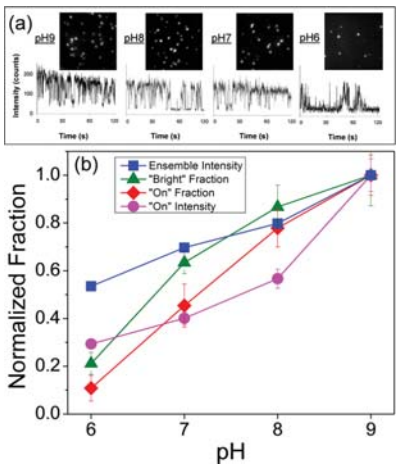

Figure 5. (a) Example single QD images from which the relative "bright" fraction, relative "on" fraction, and relative "on" intensity are extracted. The traces under each image show an example fluorescence trajectory of a single QD at the pH indicated. From ~200 of these traces, the average "On Fraction" and the average "On Intensity" is extracted, as described in the Experimental Section. (b) Comparison of the effect of pH between the ensemble and single particle fluorescence observations. Blue square symbols are the ensemble fluorescence intensity measured as the area under the fluorescence spectra of Figure 1. Green triangle symbols show the "bright fraction" of QDs in the sample, measured as the relative fraction of single QDs showing emission at some point during the whole movie. Red diamond symbols quantify the number of QDs that are "On" for a 50 ms frame, averaged over all frames (average "On Fraction"). Magenta circle symbols show the relative average "On Intensity". The data are all normalized to the QDs measured in pH 9 solution for easy comparison.

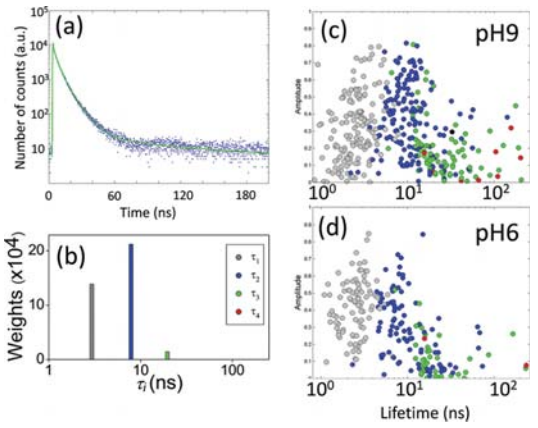

Figure 6. (a) Example fluorescence lifetime trace of a single QD at pH 6, highlighting the good signal-to-noise ratio of the signal at the single QD level. (b) Example distribution of lifetime constants recovered from a single QD. A similar histogram is extracted for ~200 single QDs. (c,d) Scatter plot of the recovered lifetime decay components and their amplitudes of ~200 single QDs at pH 6 and 9, respectively. Each point represents a recovered lifetime component and the corresponding relative amplitude for a single QD. Component colors are the same as in Figure 3.

different pH conditions. If both the "bright" fraction and the "on" fraction decrease more rapidly than the ensemble fluorescence intensity, there must be photons that contribute to the ensemble intensity measurements that are, as yet, unaccounted for in the single particle parameters. We did attempt to lower the pH below 6, but were unable to observe any QDs at the single QD level below this pH value.

We have previously found that the effect of decreasing pH on both single QD intensity and blinking was irreversible,[17] just as we observe the same pH effect on the ensemble fluorescence to be irreversible. One of the main points of this study is to determine the physical origin of these effects by measuring the changes in the fluorescence intensity and fluorescence lifetime at both the ensemble and single QD level.

Comparing pH Dependence of Fluorescence Lifetime. To connect the pH effects on the ensemble fluorescence lifetime to the single QD level, we also measured the fluorescence lifetimes of single QDs. An example of a single QD decay at pH 6 is shown in Figure 6a. Lifetime histograms obtained from single QDs are fit using the same algorithm used for the ensemble data, recovering amplitudes for a set of fixed lifetimes. While the data are a little noisier for single QDs than for the ensemble data, the signal-to-noise ratio is still high enough to recover distinct lifetimes from a single QD (Figure 6a,b). Figure 6c,d shows scatter plots of the recovered amplitudes and lifetimes for pH 9 and 6 for ~200 single QDs. Each data point represents the recovered amplitude and lifetime for each component for a single QD. All QDs showed at least two lifetime components, but most showed three components. Only a small number showed all four components that were observed in the ensemble lifetime decay (Figure 3). The important observations here are that (1) there is a wide range of lifetime components and amplitudes obtained for single QDs, suggesting broad heterogeneity at the single QD level (which appeared to be averaged out at the ensemble level); (2) QDs primarily show three lifetime components at the single QD level but show four at the ensemble level; and (3) the contribution from longer lifetime components is slightly less at pH 9 than at pH 6, in contrast to the results obtained at the ensemble level.

DISCUSSION

A comprehensive model that connects and rationalizes the single molecule and ensemble optical properties of QDs has yet to be fully elucidated. A central aim of this study is to bridge this gap by observing how several distinct but physically connected optical properties are affected by changes in solution pH. In particular, the effects of pH on the measured fluorescence intensity and lifetime, together with our previous report on blinking,[17] at both the ensemble and single QD level highlight that the single QD properties contribute to the ensemble properties in a nontrivial manner.

Comparison of the pH Effect on Blinking, Dark Fraction, and Ensemble Intensity. We previously analyzed in detail the

effect of pH on the blinking statistics and the formation of the dark fraction.[17] In this study, we extend the analysis to attempt to quantify the relationship of these properties to the ensemble fluorescence intensity. Figure 5 showed that the ensemble fluorescence intensity, the number of emitting ("bright") QDs and the average "on" fraction (the fraction of emitting QDs that are "on" at a given time) decreased rapidly, nonlinearly, and nonconcomitantly with decreasing pH of the solution. These results highlight the fact that the ensemble quantum yield of QDs is not solely determined by the bright to dark fraction ratio[13,15] but is much more complicated. A detailed comparison of the pH dependence on these properties leads to an interesting quandary. Between pH 9 and 8, the ensemble fluorescence intensity decreased concomitantly with the decrease in the average "on" fraction as a result of the pH influence on blinking statistics.[17] However, below pH 8, both the "bright" fraction and the "on" fraction decrease much more rapidly than the ensemble fluorescence intensity. Our previous report had observed that the brightness of the "on" state decreases between pH 9 and 6.[17] If the "bright fraction", the "on fraction", and the "on brightness", all decrease more quickly than the ensemble fluorescence intensity, and this leads to the conclusion that there are photons that are, as yet, unaccounted for in the single particle parameters that contribute to the ensemble fluorescence.

Before we attempt to account for these photons, it will be useful to postulate the microscopic origins of the irreversible decrease in the fluorescence and then relate them to the decrease in the "bright" and "on" fractions, as well as the fluorescence lifetime decays.

Possible Origins of the Irreversible Decrease in QD Ensemble Fluorescence with Decreasing pH. The effect of pH on the fluorescence intensity and dark fraction was found to be irreversible. For example, immersing QDs in pH 9 solution after being exposed to pH 6 did not recover the fluorescence. An irreversible decrease in the ensemble fluorescence intensity of CdTe–ZnS core–shell QDs with decreasing pH was previously reported,[41] although the exact dependence was different than those reported here and was accompanied by a spectral red shift. Another report on CdSe–ZnS core–shell QDs reported an oxygen-dependent decrease in the ensemble fluorescence, but it was accompanied by a spectral blue shift.[47,48] Our results show the involvement of both H^+ ions and O_2 in the fluorescence intensity decrease, but the fact that there is no spectral shift associated with the decay suggests that the core size was unaffected by pH, and that any chemical changes must have occurred only in the shell, or possibly at the core–shell interface.

It is safe to assume that the low-density organic passivating layers of the QD are easily penetrated by both H^+ and O_2. We previously analyzed the homogeneity and isotropy of the QD shell by TEM[17] and found that the QD shell was rod-like rather than spherical, highlighting the anisotropic structure of the ZnS shell (Supporting Information). Other reports of commercially available QDs have also shown similar anisotropic shell structures.[51] From the TEM images of the particles used in this study, we estimate that the thickness of the ZnS shell varies from 1 to more than 4 monolayers both within individual QDs and across the ensemble. It is likely that the structure of the shell changes from crystalline in thicker areas to an amorphous phase, typical for thin regions, allowing a higher chemical sensitivity to the surrounding environment. We now consider possible chemical changes of the ZnS shell, which can lead to formation of trap states and how they can affect the optical properties of QDs.

ZnS is very thermodynamically stable under normal conditions; the dissociation of ZnS directly into Zn^{2+} and S^{2-} has a $\Delta G = +139.4$ kJ mol^{-1}.[52] However, in the presence of acid and oxygen, the reaction

$$ZnS_{(s)} + 2H^+_{(aq)} + 1/2O_{2(aq)} \rightarrow S_{(s)} + Zn^{2+}_{(aq)} + H_2O_{(l)} \quad (1)$$

has a $\Delta G = -81$ kJ mol^{-1},[52,53] and a relatively low activation energy, $E_a = 25$ kJ mol^{-1},[54] highlighting that the reaction is diffusion-controlled and thus would be highly dependent on pH and O_2. We postulate that the ZnS shell may be exposed to slow decomposition, possibly exposing the CdSe core in regions where the shell is particularly thin. Several factors can be expected to limit this decomposition process: (1) the low solubility of O_2 in water, (2) the poor solubility of elemental sulfur in water; (3) the fact that $[H^+]$ is limited at pH 6 (note: we did lower the pH below 6 but were unable to observe any single QD fluorescence). Another interesting potential limitation to the decomposition may arise from (4) the formation of a chemically benign layer at the shell outer surface. Recent studies[55] on the oxidation of FeS in oxygen-bearing acidic solutions proposed a mechanism by which oxidative dissolution of FeS starts by proton binding and attack to the surface-bound S^{2-}. We will subsequently refer to surface-bound S^{2-} as $>S^{2-}$, highlighting the fact that the S atom remains bound to the surface of the nanocrystal. A similar mechanism may arise in the ZnS shell to form surface $>SH_2$ sites, which could then transform into $>S^{2-}_m$ by reaction with O_2 and release of Zn^{2+}. We then propose that the polysulfide groups form a poorly ordered sulfur-rich layer (SRL), inhibiting further Zn^{2+} dissolution as follows:

$$(>S^{2-})_{QD} + 2H^+_{(aq)} \Leftrightarrow (>SH_2)_{QD} \quad (2)$$

$$x(>SH_2)_{QD} + \frac{x}{2}\left(1 - \frac{1}{y}\right)O_{2(aq)} \Leftrightarrow \frac{x}{y}(S^{2-}_m)_{QD} + x\left(1 - \frac{1}{y}\right)H_2O_{(l)} + 2\frac{x}{y}H^+_{(aq)} \quad (3)$$

The formation of $>S_m^{2-}$ (SRL) is a self-inhibiting process due to the fact that, once formed, it would block access of O_2 and H^+ to react with more ZnS. This would lead to a saturation point in the extent of reaction. Figure 3 is consistent with this saturation effect since it exhibits a leveling off of the fluorescence intensity with time of exposure to the pH-adjusted salt solution, dependent on both pH and O_2, providing support for one of the reaction limitations described above. The limitation is also consistent with the fact that we saw no changes in the fluorescence peak position as a function of pH, thus restricting the reactions to the shell but not penetrating to the core. It is, as yet, open for further study whether the oxidation does indeed proceed with the formation of the SRL ($>S_m^{2-}$) or elemental sulfur, S^0. Still, due to the insolubility of S^0 in water and the difficulty in forming the stable S_8 allotrope without significant lattice rearrangement, if any elemental sulfur does form, it likely remains bound to the surface of the QD. X-ray photoelectron spectroscopy (XPS) should provide a way to address this issue in future studies. If formed, further oxidation of $S_{(s)}$ to $SO_{2(g)}$ is thermodynamically allowed ($\Delta G_f(SO_2) = -300.1$ kJ mol^{-1}) but is very slow and may eventually dissolve in water to form bisulfite and sulfite by

$$S_{(s)} + O_{2(aq)} \rightarrow SO_{2(g)} \quad (4)$$

$$SO_{2(g)} + H_2O_{(l)} \rightarrow HSO_{3(aq)}^- + H_{(aq)}^+ \overset{pK_a 7.0}{\leftrightarrow} SO_{3(aq)}^{2-} + 2H_{(aq)}^+ \quad (5)$$

Thus, over extended periods of time, sections of the shell can decompose in the presence of acid and oxygen, but it is unlikely that much SO_2 will be released under these experimental conditions.

Furthermore, the rates of all these reactions will be accelerated under illumination. In accordance with the electron-active photooxidation model,[56,57] excitonic wave functions that tunnel into the thin areas of the ZnS shell catalyze the dissociation of molecular oxygen into oxygen radicals. This is in agreement with our observations since the effect of pH on single QD intensity values was more pronounced when the QDs were exposed to laser illumination. For example, during the time it took to collect one single QD image sequence at pH 6 (~5 min), almost all initially emitting dots on the glass surface became dark; however, switching to a new nonirradiated observation area on the sample after the initial 5 min acquisition revealed that many of the QDs in the new region were still capable of emitting. Similar experiments on different batches of commercial CdSe–ZnS core–shell QDs from different sources showed the same trend with pH as shown in Figure 3, but the time scales and extents of the fluorescence intensity decay varied from batch to batch (results not shown). These observations suggest that differences in the shell quality from different batches play a role in the variations observed in the pH dependence of the QD emission.

Relating the Postulated Chemical Changes to the Blinking, Dark Fraction, and Fluorescence Lifetime. Of the various possible (and structurally complex) forms that sulfur can exist on the QD shell surface, some of them could act as trap states for the exciton charge carriers (most likely for the hole), particularly for the binding of H^+ to the surface and in the formation of a poorly ordered SRL. Furthermore, in the environment of the QD surface, where the polymeric stabilizing ligands contain complex-forming moieties (such as C=O or N–H groups), dissociated Zn^{2+} may not even enter the solution as free ions but may remain closely associated with the QD surface and may also be involved in a trap-state role (most likely for the electrons). These various trap states could alter both radiative and nonradiative relaxation rates, as well as affecting the blinking statistics.

Our previous studies led us to hypothesize that there was an intrinsic connection between the blinking mechanism and the mechanism of dark fraction formation.[17] We interpreted the pH effect on blinking as the H^+ ions interacting with the shell surface to facilitate the trapping of charge carriers, which has been associated with the "off" state.[33,58–61] Wang has calculated the effect of external charges on the optical properties of QDs.[62] In addition to the electrostatic effect of the H^+ ions, the fact that the reduction in fluorescence intensity of the QDs was irreversible after the pH was lowered leads us to the conclusion that the chemical reactions described above would lead to a permanent change in the trap states that affects the blinking, fluorescence intensity, and dark fraction.

Trap state formation also affects fluorescence lifetimes. In a recent study by Jones *et al.*, the authors used Marcus theory to show the presence of two types of trap states: one localized on the outermost ZnS surface and another trap state nearer to the CdSe core at the core–shell interface.[18] We will refer to them here as "shell traps" and "interface traps", respectively. While their experiments were carried out in organic solvents, and our experiments were carried out in aqueous solutions, the data of Figure 4 show remarkably similar lifetime components to the Jones *et al.* study (without *a priori* assuming the number of exponentials in the decays); τ_2 is consistent with the intrinsic decay time of the delocalized exciton observed by Jones *et al.*, and τ_3 is consistent with the lifetime that was assigned to interface traps.[18] The fastest lifetime component is small in amplitude for the ensemble experiments but larger in amplitude for the experiments on single QDs. The single QD experiments are conducted under much higher photon flux than the ensemble experiments, which leads us to suspect that the fast lifetime component is due to trion or multiexciton decay, which has

been shown to be approximately 1−2 ns or faster, depending on the conditions.[63,64] The fact that this fast component appears to be power-dependent and not pH-dependent supports this assignment.

The longest lifetime component, τ_4, was the only one found to be pH-dependent. At pH 9, τ_4 was ∼80 and ∼160 ns at pH 6 (Figure 3c). In pH 9 solution, τ_4 gradually increased over time from 42.8 ± 6.2 ns during the first 10 min to 118.7 ± 23.9 ns in the last 10 min (Figure 4a,b). When the QDs were immersed in pH 6 solution, τ_4 was initially measured to be ∼159 ± 7 ns during the first 10 min and slowly rose to ∼172 ± 10 ns in the last 10 min. In pH 6 solution, there is a difference in the time dependence of the intensity change (Figure 2) and the time dependence of the τ_4 lifetime component change (Figure 4). The lifetime component τ_4 changes significantly faster than the intensity changes. We hypothesize this difference to be the result of the initial environmental change of H^+ ions surrounding the QD, affecting τ_4 but not significantly reducing the fluorescence intensity. As time proceeds, the chemical reactions described above introduce permanent changes in the shell surface that causes the QDs to first increase their blinking and then form a dark fraction, with only small additional changes in the τ_4 component (which had already changed significantly due to the presence of H^+ ions). In contrast, at pH 9, the immediate environmental effect of the H^+ ions is negligible. The low concentration of H^+ ions in solution with the presence of O_2 will cause the chemical reactions at the shell surface to be much slower, eventually introducing trap states that affect blinking, dark fraction formation, and τ_4 over longer periods of time. Future experiments will further probe the effect of O_2 on the fluorescence lifetime components at both the ensemble and single QD level.

Extra Photons Detected in the Ensemble Fluorescence Intensity. Strikingly, single QD lifetime measurements do not show a significant τ_4 component. Figure 6 shows the analysis of ∼200 single QDs at pH 9 and 6, for which only a small fraction showed a τ_4 component. Most single QDs recovered two or three components. The τ_1 and τ_2 components are the same at pH 6 and 9, with only minor differences observed in the long time scale components. This effectively shows that, at the single QD level, the average fluorescence lifetime of QDs at pH 6 is shorter than at pH 9, while at the ensemble level, the average fluorescence lifetime of QD at pH 6 is longer than at pH 9. From this difference, we conclude that the long lifetime component present in the ensemble data, which increases at lower pH, originates from QDs not observed in single QD experiments. This implies that the dark fraction of QDs is emitting photons with a long lifetime component, but that the number of photons emitted is too low for detection above the background in the single QD measurements. In typical single molecule experiments, a threshold is

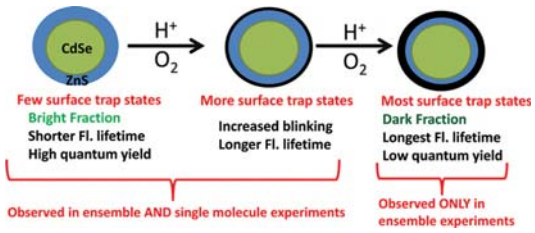

Figure 7. Model of the pH dependence on the QD shell surface. The formation of trap states initially causes increased blinking and longer fluorescence lifetimes but then leads to the QD becoming permanently dark. These dark QDs are unobserved in single molecule measurements but contribute to the ensemble measurements.

set that determines if a QD is bright or dark (and therefore observed) taking into account the signal-to-noise ratio of the experimental setup. However, ensemble-averaged data have no such threshold and can therefore integrate contributions from dim QDs, that is, still emitting but categorized as "off" (dark) in single QD experiments. This model is summarized in Figure 7, highlighting that the formation of trap states first leads to increased blinking and then to a "dark" fraction that cannot be observed in single QD measurements but still emits photons which contribute to the integrated ensemble signal.

This interpretation provides an explanation for the lack of observation of the long lifetime component in many QDs at low pH in the single molecule data, whereas it is observed at the ensemble level. The observation of the few QDs with a τ_4 component may be attributed to those with significant "off" periods in their blinking dynamics, connected with our earlier hypothesis of the dark fraction formation resulting from the same mechanism as the "off" state during blinking.[17] Rosen *et al.*[61] and the Bawendi group[65] have recently brought into question the long-standing assumption that the "off" state is the result of Auger recombination, and other recent reports have observed that the "off" state does in fact emit photons.[66,67] Rosen *et al.*[61] further found that the lifetime of the "off" state is multiexponential. By monitoring the power dependence of the "off" state lifetime, they concluded that the "off" state lives longer than the exciton radiative lifetime. The pH-dependent long lifetime component that we observed here supports their interpretation, further showing that this long lifetime component is affected by the environment. If the "off" state occurs due to long time scale trapping at the shell surface traps, it can be expected to be pH-dependent. At first, it may seem counterintuitive that a lower quantum yield state leads to a longer fluorescence lifetime, τ_{fl}, since it is expected that increasing the nonradiative decay rate (k_{NR}) should reduce the fluorescence lifetime by the relationship

$$k_{fl} = \frac{1}{\tau_{fl}} = k_R + k_{NR} \qquad (6)$$

which usually assumes that the radiative decay rate, k_R, is constant. However, it has been observed that the external environment can also significantly alter k_R.[31] This may be understood as trapping of one of the charge carriers at the shell surface which reduces the overlap integral of the electron and hole wave functions, thus decreasing the radiative rate for that process (component). If the decrease in k_R is larger than the increase in the k_{NR}, then τ_{fl} would increase for that component.

It should be noted that, in addition to excitation power, the excitation wavelength has been shown to affect blinking[68,69] and fluorescence lifetime.[12] Our excitation energies are high above the band gap of the QDs. By using an excitation laser source closer in energy to the band gap, it may be possible to reduce the contribution of the trap state emission, thereby reducing the pH dependence. Unfortunately, at the present time, we are unable to examine this effect due to limitations in the availability of such lasers in our lab. Differences in the blinking and quantum yield measured for QDs in solution and immobilized on a surface may also be affected by an applied electric field on the order of tens to hundreds of millivolts.[70] Possible fluctuating electric fields due to charge dynamics in immobilized QDs may also be involved but would be difficult to quantify. However, in order to significantly affect the dynamics, these fluctuating fields would need to be quite strong.

Finally, it should be noted that TEM for these[17] and other[51] QDs show that core−shell samples are not always spherical. Example TEM images of these QDs are given in the Supporting Information, highlighting their nonspherical shape. In thin regions of the shell, interface trap states and shell-surface trap states may begin to overlap. This overlap could explain our observed strong pH dependence on blinking, dark fraction, and fluorescence lifetime, which may not be as prevalent for QDs with thick isotropic shells, which have shown reduced blinking.[34,35]

CONCLUSION

By comparing the ensemble fluorescence intensity to the average "on" and "bright" fractions from single particle measurements, we identified the presence of photons detected at the ensemble level that are not observed at the single QD level. Fluorescence lifetime analysis shows multiexponential behavior but with a different pH dependence at the ensemble level as compared to the single QD level. We have uncovered two effects of pH: a physical effect of charges surrounding the QD and an irreversible chemical effect from reaction of the H^+ and O_2 with the QD surface. We have hypothesized chemical reactions that can occur at the shell surface and result in the formation of charge carrier trap states. Finally, we have connected these trap states to the blinking, dark fraction, and fluorescence lifetime components and show evidence that the dark fraction emits photons with long lifetime but low quantum efficiency.

This paper highlights the point that the ensemble quantum yield cannot be estimated just by observing the dark fraction but must also include analysis of blinking, multiexponential fluorescence lifetime, and single particle brightness. In order to understand the microscopic basis for the observed fluorescence properties, it is important to monitor the interplay between these properties at both the single QD and ensemble level. These results will have important implications for QD-based fluorescence lifetime imaging (FLIM), which has been shown to be particularly promising for QDs due to their relatively long fluorescence lifetimes, as well as for proper quantitative interpretation of fluorescence microscopy studies that employ QD-tagged biomolecules in cells.

EXPERIMENTAL SECTION

Samples and Instrumentation. Samples of CdSe/ZnS QDs were purchased from Invitrogen Canada Inc. (Burlington, ON). We used CdSe/ZnS quantum dots (QD605-streptavidin) that were coated in a poly(acrylic acid)-based amphiphilic polymer and subsequently functionalized with streptavidin, having their emission wavelength centered at 605 nm. To prepare pH-adjusted salt solutions with values ranging from 9 to 6, dilute HCl or NaOH was added to dissolved PBS preparations (Fisher Scientific, Pittsburgh, PA) with fixed concentrations of NaCl (150 mM) and Na_3PO_4 (20 mM).

Samples for ensemble emission experiments were prepared by diluting the QD stock solution (2 μM) $\sim 10^3$-fold in pH-adjusted PBS solutions and placed in cuvettes immediately prior to data collection. Fluorescence emission spectra and intensity decays were measured on a Thermo Spectronic spectrofluorometer, Aminco-Bowman series 2 (Rochester, NY, USA). Emission spectra were collected with 1 nm spectral resolution in the range of 550−700 nm. Intensity decays were measured by sampling the emission intensity at 605 nm every 1 s for 6000 s. The nanosecond fluorescence lifetime histograms were measured using the time-correlated single photon counting (TCSPC) method. As a pulsed excitation source, we used a PDL 800B diode-pumped solid-state (DPSS) laser (Picoquant, Berlin, Germany) with emission wavelength at 407 nm, pulse width 70 ps, operating at a repetition rate of 2.5 MHz. Data were acquired on a TCSPC acquisition card (TimeHarp 200, PicoQuant) to record decay kinetics in 2900 channels with 144 ps per channel.

Samples for single QD experiments were prepared by attachment of QDs to a glass surface as previously described.[17] Briefly, microscope coverslips (Fisher Scientific, No. 1) were first cleaned in Piranha solution (3:1 concentrated sulfuric acid/30% hydrogen peroxide) and then amino-functionalized with 3-aminopropyltriethoxylsilane (Pierce, Rockford, IL). Next, the amino groups were modified with a 10 mM aqueous Sulfo-LC-SPDP solution (Pierce, Rockford, IL) and exposed to reduced biotinylated BSA (Pierce, Rockford, IL) to form covalent bonds with the protein. The QD605-streptavidin stock solution (2 μM) was diluted by a factor of 10^6 in MilliQ water (>18 M$\Omega \cdot$cm^{-1}) and sonicated for 15 min prior to deposition on biotinylated glass.

For imaging experiments, PBS salt solutions of a given pH were added directly to the glass-immobilized QDs and the samples imaged immediately afterward. Since the pH effect was found to be irreversible, each pH experiment used a new sample preparation. At least three preparations at each pH were used to reduce sampling errors.

For single QD fluorescence intensity measurements, images of spatially resolved individual streptavidin-QDs deposited on a BSA-biotin-coated glass surface were recorded on a home-built objective-type total internal reflection fluorescence microscope (TIRFM) equipped with an intensified PentaMax charge-coupled device (CCD) camera (Princeton Instruments, Trenton, NJ) as previously described.[17] The 488 nm line from an Ar^+ laser (Melles Griot 35 LAP 431) was used for evanescent wave sample boundary excitation through a Zeiss Planapo 100×, 1.45 NA objective lens. Fluorescence from the sample was collected with the same objective and filtered with an emission filter D605/55 nm (Chroma Technology, Rockingham, VT). Image time series containing 2000 frames were collected with 50 ms frame time resolution.

For single QD lifetime measurements, images of spatially resolved individual streptavidin-QDs deposited on a BSA-biotin-coated glass surface were recorded using a scanning confocal fluorescence lifetime imaging microscope (MicroTime 200, Picoquant) consisting of a pulsed 485 nm DPSS laser (LDH-D-C-485), pulse width 70 ps, operating at a repetition rate of 5 MHz and data acquired by a TCSPC card (PicoHarp 300) in 4096 channels with 128 ps per channel to ensure complete decay in between pulses.

Data Analysis. Analysis of the fluorescence intensity from spatially resolved QDs was performed in ImageJ as previously described.[17,33,71] To determine the average QD "on" intensity, the intensity for each resolved QD was recorded for each frame over a total of 2000 frame time series to obtain intensity−time trajectories for each QD. Each time point below the "on"−"off" threshold was discarded, then the average intensity (and standard deviation) of the remaining time points determined. This analysis provided the average "on" intensity of a single QD independent of its blinking statistics, provided the QD was on for at least one frame. In order to measure the "dark fraction", each QD that had at least one frame with an intensity value over the "on"−"off" threshold value was counted as a "bright" quantum dot. This was compared to the "bright" fraction at pH 9, and the difference was assigned as the (relative) "dark" fraction. The average "on" fraction was determined by finding the number of QDs that were "on" in a given frame and dividing it by the "bright" fraction, repeated over all frames. From these data, the average value and standard deviation of the average "on" fraction were computed.

Processing of fluorescence lifetime data was done using a publically available Matlab routine[49] developed by Enderlein.[50] The algorithm is capable of fitting and performing numerical reconvolution to account for the finite instrument response function. The algorithm is particularly well suited to fitting multiexponential decay curves of the form of eq 7 by avoiding the pitfall of simultaneously fitting the amplitudes and decay times using least-squares fitting of a predetermined number of exponents.

$$I = \sum_i a_i e^{-t/\tau_i} \tag{7}$$

where τ_i and a_i are, respectively, the decay times and the corresponding number of photons that come from process i in the multiexponential decay model. The amplitudes and lifetimes of each component have a high dependence on each other and are highly sensitive to the initial parameter guesses using a typical Marquardt−Levenberg least-squares fitting minimization.[50] This pitfall is avoided by assigning fixed values of a large number of lifetime components and performing a maximum likelihood estimation of the amplitude parameters. We assigned 100 fixed values to parameters τ_i spanning the range τ_1 = channel resolution to τ_{100} = total acquisition time, distributed equally as log(τ), and recover the nonzero a_i coefficients. This type of analysis results in a histogram of characteristic exponential decay times weighted according to their contribution to the fit.

Acknowledgment. C.D.H. would like to acknowledge generous financial support from the NIH NCRR COBRE Grant P30 RR031154-01, the Arkansas Biosciences Institute, and the University of Arkansas. P.W.W. and P.G. acknowledge support from the Natural Sciences and Engineering Research Council of Canada (NSERC), Canadian Institutes of Health Research (CIHR), and Le Fonds Québécois de la Recherche sur la Nature et les Technologies (FQRNT). P.G. acknowledges Canadian Institute for Advanced Research (CIfAR).

Supporting Information Available: QD absorption spectra, effects of salt ions on fluorescence quenching and TEM images. This material is available free of charge *via* the Internet at http://pubs.acs.org.

REFERENCES AND NOTES

1. Murray, C. B.; Norris, D. J.; Bawendi, M. G. Synthesis and Characterization of Nearly Monodisperse CdE (E = Sulfur, Selenium, Tellurium) Semiconductor Nanocrystallites. *J. Am. Chem. Soc.* **1993**, *115*, 8706–8715.
2. Talapin, D. V.; Rogach, A. L.; Kornowski, A.; Haase, M.; Weller, H. Highly Luminescent Monodisperse CdSe and CdSe/ZnS Nanocrystals Synthesized in a Hexadecylamine-Trioctylphosphine Oxide-Trioctylphospine Mixture. *Nano Lett.* **2001**, *1*, 204–211.
3. Peng, Z. A.; Peng, X. Formation of High-Quality CdTe, CdSe, and CdS Nanocrystals Using CdO as Precursor. *J. Am. Chem. Soc.* **2001**, *123*, 183–184.
4. Li, J. J.; Wang, Y. A.; Guo, W.; Keay, J. C.; Mishima, T. D.; Johnson, M. B.; Peng, X. Large-Scale Synthesis of Nearly Monodisperse CdSe/CdS Core/Shell Nanocrystals Using Air-Stable Reagents *via* Successive Ion Layer Adsorption and Reaction. *J. Am. Chem. Soc.* **2003**, *125*, 12567–12575.
5. Chan, W. C.; Nie, S. Quantum Dot Bioconjugates for Ultrasensitive Nonisotopic Detection. *Science* **1998**, *281*, 2016–2018.
6. Bruchez, M., Jr.; Moronne, M.; Gin, P.; Weiss, S.; Alivisatos, A. P. Semiconductor Nanocrystals as Fluorescent Biological Labels. *Science* **1998**, *281*, 2013–2016.
7. Akerman, M. E.; Chan, W. C.; Laakkonen, P.; Bhatia, S. N.; Ruoslahti, E. Nanocrystal Targeting *in Vivo*. *Proc. Natl. Acad. Sci. U.S.A.* **2002**, *99*, 12617–12621.
8. Wu, X.; Liu, H.; Liu, J.; Haley, K. N.; Treadway, J. A.; Larson, J. P.; Ge, N.; Peale, F.; Bruchez, M. P. Immunofluorescent Labeling of Cancer Marker Her2 and Other Cellular Targets with Semiconductor Quantum Dots. *Nat. Biotechnol.* **2003**, *21*, 41–46.
9. Alivisatos, A. P. The Use of Nanocrystals in Biological Detection. *Nat. Biotechnol.* **2004**, *22*, 47–52.
10. Michalet, X.; Pinaud, F. F.; Bentolila, L. A.; Tsay, J. M.; Doose, S.; Li, J. J.; Sundaresan, G.; Wu, A. M.; Gambhir, S. S.; Weiss, S. Quantum Dots for Live Cells, *In Vivo* Imaging, and Diagnostics. *Science* **2005**, *307*, 538–544.
11. Nirmal, M.; Brus, L. Luminescence Photophysics in Semiconductor Nanocrystals. *Acc. Chem. Res.* **1999**, *32*, 407–414.
12. Meijerink, A. Exciton Dynamics and Energy Transfer Processes in Semiconductor Nanocrystals. In *Semiconductor Nanocrystal Quantum Dots: Synthesis, Assembly, Spectroscopy and Applications*; Rogach, A. L., Ed.; Springer: Vienna, 2008; pp 277−310.
13. Ebenstein, Y.; Mokari, T.; Banin, U. Fluorescence Quantum Yield of CdSe/ZnS Nanocrystals Investigated by Correlated Atomic-Force and Single-Particle Fluorescence Microscopy. *Appl. Phys. Lett.* **2002**, *80*, 4033–4035.
14. Brokmann, X.; Coolen, L.; Dahan, M.; Hermier, J. P. Measurement of the Radiative and Non-radiative Decay Rates of Single CdSe Nanocrystals through Controlled Modification of Their Spontaneous Emission. *Phys. Rev. Lett.* **2004**, *93*, 107403.
15. Yao, J.; Larson, D. R.; Vishwasrao, H. D.; Zipfel, W. R.; Webb, W. W. Blinking and Nonradiant Dark Fraction of Water-Soluble Quantum Dots in Aqueous Solution. *Proc. Natl. Acad. Sci. U.S.A.* **2005**, *102*, 14284–14289.

16. Gao, X.; Chan, W. C. W.; Nie, S. Quantum-Dot Nanocrystals for Ultrasensitive Biological Labeling and Multicolor Optical Encoding. *J. Biomed. Opt.* **2002**, *7*, 532–537.
17. Durisic, N.; Wiseman, P. W.; Grütter, P.; Heyes, C. D. A Common Mechanism Underlies the Dark Fraction Formation and Fluorescence Blinking of Quantum Dots. *ACS Nano* **2009**, *3*, 1167–1175.
18. Jones, M.; Lo, S. S.; Scholes, G. D. Quantitative Modeling of the Role of Surface Traps in CdSe/CdS/ZnS Nanocrystal Photoluminescence Decay Dynamics. *Proc. Natl. Acad. Sci. U.S.A.* **2009**, *106*, 3011–3016.
19. Pokrant, S.; Whaley, K. B. Tight-Binding Studies of Surface Effects on Electronic Structure of CdSe Nanocrystals: The Role of Organic Ligands, Surface Reconstruction, and Inorganic Capping Shells. *Eur. Phys. J. D* **1999**, *6*, 255–267.
20. Nirmal, M.; Murray, C. B.; Bawendi, M. G. Fluorescence-Line Narrowing in CdSe Quantum Dots: Surface Localization of the Photogenerated Exciton. *Phys. Rev. B* **1994**, *50*, 2293.
21. Kapitonov, A. M.; Stupak, A. P.; Gaponenko, S. V.; Petrov, E. P.; Rogach, A. L.; Eychmueller, A. Luminescence Properties of Thiol-Stabilized CdTe Nanocrystals. *J. Phys. Chem. B* **1999**, *103*, 10109–10113.
22. Underwood, D. F.; Kippeny, T.; Rosenthal, S. J. Charge Carrier Dynamics in CdSe Nanocrystals: Implications for the Use of Quantum Dots in Novel Photovoltaics. *Eur. Phys. J. D* **2001**, *16*, 241–244.
23. Baker, D. R.; Kamat, P. V. Tuning the Emission of CdSe Quantum Dots by Controlled Trap Enhancement. *Langmuir* **2010**, *26*, 11272–11276.
24. Jones, M.; Scholes, G. D. On the Use of Time-Resolved Photoluminescence as a Probe of Nanocrystal Photoexcitation Dynamics. *J. Mater. Chem.* **2010**, *20*, 3533–3538.
25. Breus, V. V.; Heyes, C. D.; Nienhaus, G. U. Quenching of CdSe−ZnS Core−Shell Quantum Dot Luminescence by Water-Soluble Thiolated Ligands. *J. Phys. Chem. C* **2007**, *111*, 18589–18594.
26. Khatchadourian, R.; Bachir, A.; Clarke, S. J.; Heyes, C. D.; Wiseman, P. W.; Nadeau, J. L. Fluorescence Intensity and Intermittency as Tools for Following Dopamine Bioconjugate Processing in Living Cells. *J. Biomed. Biotechnol.* **2007**, *2007*, 70145.
27. Landes, C. F.; Burda, C.; Braun, M.; El-Sayed, M. A. Photoluminescence of CdSe Nanoparticles in the Presence of a Hole Acceptor: *n*-Butylamine. *J Phys. Chem. B* **2001**, *105*, 2981–2986.
28. Munro, A. M.; Ginger, D. S. Photoluminescence Quenching of Single CdSe Nanocrystals by Ligand Adsorption. *Nano Lett.* **2008**, *8*, 2585–2590.
29. Hohng, S.; Ha, T. Near-Complete Suppression of Quantum Dot Blinking in Ambient Conditions. *J. Am. Chem. Soc.* **2004**, *126*, 1324–1325.
30. Heuff, R. F.; Marrocco, M.; Cramb, D. T. Saturation of Two-Photon Excitation Provides Insight into the Effects of a Quantum Dot Blinking Suppressant: A Fluorescence Correlation Spectroscopy Study. *J. Phys. Chem. C* **2007**, *111*, 18942–18949.
31. Fomenko, V.; Nesbitt, D. J. Solution Control of Radiative and Nonradiative Lifetimes: A Novel Contribution to Quantum Dot Blinking Suppression. *Nano Lett.* **2008**, *8*, 287–293.
32. Cooper, D. R.; Suffern, D.; Carlini, L.; Clarke, S. J.; Parbhoo, R.; Bradforth, S. E.; Nadeau, J. L. Photoenhancement of Lifetimes in CdSe/ZnS and CdTe Quantum Dot−Dopamine Conjugates. *Phys. Chem. Chem. Phys.* **2009**, *11*, 4298–4310.
33. Heyes, C. D.; Kobitski, A. Y.; Breus, V. V.; Nienhaus, G. U. Effect of the Shell on Blinking Statistics in Single Core−Shell Quantum Dots: A Single Particle Fluorescence Study. *Phys. Rev. B* **2007**, *75*, 125431.
34. Chen, Y.; Vela, J.; Htoon, H.; Casson, J. L.; Werder, D. J.; Bussian, D. A.; Klimov, V. I.; Hollingsworth, J. A. "Giant" Multishell CdSe Nanocrystal Quantum Dots with Suppressed Blinking. *J. Am. Chem. Soc.* **2008**, *130*, 5026–5027.
35. Mahler, B.; Spinicelli, P.; Buil, S.; Quelin, X.; Hermier, J. P.; Dubertret, B. Towards Non-blinking Colloidal Quantum Dots. *Nat. Mater.* **2008**, *7*, 659–664.
36. Wang, X.; Ren, X.; Kahen, K.; Hahn, M. A.; Rajeswaran, M.; Maccagnano-Zacher, S.; Silcox, J.; Cragg, G. E.; Efros, A. L.; Krauss, T. D. Non-blinking Semiconductor Nanocrystals. *Nature* **2009**, *459*, 686–689.
37. Boldt, K.; Bruns, O. T.; Gaponik, N.; Eychmueller, A. Comparative Examination of the Stability of Semiconductor Quantum Dots in Various Biochemical Buffers. *J. Phys. Chem. B* **2006**, *110*, 1959–1963.
38. Sun, Y. H.; Liu, Y. S.; Vernier, P. T.; Liang, C. H.; Chong, S. Y.; Marcu, L.; Gundersen, M. A. Photostability and pH Sensitivity of CdSe/ZnSe/ZnS Quantum Dots in Living Cells. *Nanotechnology* **2006**, *17*, 4469–4476.
39. Liu, Y.-S.; Sun, Y.; Vernier, P. T.; Liang, C.-H.; Chong, S. Y. C.; Gundersen, M. A. pH-Sensitive Photoluminescence of CdSe/ZnSe/ZnS Quantum Dots in Human Ovarian Cancer Cells. *J. Phys. Chem. C* **2007**, *111*, 2872–2878.
40. Deng, Z.; Zhang, Y.; Yue, J.; Tang, F.; Wei, Q. Green and Orange CdTe Quantum Dots as Effective pH-Sensitive Fluorescent Probes for Dual Simultaneous and Independent Detection of Viruses. *J. Phys. Chem. B* **2007**, *111*, 12024–12031.
41. Yu, D.; Wang, Z.; Liu, Y.; Jin, L.; Cheng, Y.; Zhou, J.; Cao, S. Quantum Dot-Based pH Probe for Quick Study of Enzyme Reaction Kinetics. *Enzyme Microb. Technol.* **2007**, *41*, 127–132.
42. Sato, K.; Kojima, S.; Hattori, S.; Chiba, T.; Ueda-Sarson, K.; Torimoto, T.; Tachibana, Y.; Kuwabata, S. Controlling Surface Reactions of CdS Nanocrystals: Photoluminescence Activation, Photoetching and Photostability under Light Irradiation. *Nanotechnology* **2007**, *18*, 465702.
43. Tomasulo, M.; Yildiz, I.; Raymo, F. M. pH-Sensitive Quantum Dots. *J. Phys. Chem. B* **2006**, *110*, 3853–3855.
44. Jin, T.; Sasaki, A.; Kinjo, M.; Miyazaki, J. A Quantum Dot-Based Ratiometric pH Sensor. *Chem. Commun.* **2010**, *46*, 2408–2410.
45. Zhang, Q.; Cao, Y.-Q.; Tsien, R. W. Quantum Dots Provide an Optical Signal Specific to Full Collapse Fusion of Synaptic Vesicles. *Proc. Natl. Acad. Sci. U.S.A.* **2007**, *104*, 17843–17848.
46. Zhang, Q.; Li, Y.; Tsien, R. W. The Dynamic Control of Kiss-and-Run and Vesicular Reuse Probed with Single Nanoparticles. *Science* **2009**, *323*, 1448–1453.
47. van Sark, W.; Frederix, P.; van den Heuvel, D. J.; Bol, A. A.; van Lingen, J. N. J.; Donega, C. D.; Gerritsen, H. C.; Meijerink, A. Time-Resolved Fluorescence Spectroscopy Study on the Photophysical Behavior of Quantum Dots. *J. Fluoresc.* **2002**, *12*, 69–76.
48. van Sark, W. G. J. H. M.; Frederix, P. L. T. M.; Van den Heuvel, D. J.; Gerritsen, H. C.; Bol, A. A.; van Lingen, J. N. J.; de Mello Donegá, C.; Meijerink, A. Photooxidation and Photobleaching of Single CdSe/ZnS Quantum Dots Probed by Room-Temperature Time-Resolved Spectroscopy. *J. Phys. Chem. B* **2001**, *105*, 8281–8284.
49. http://www.joerg-enderlein.de/research/resources/tcspcfit-a-matlab-package.html.
50. Enderlein, J.; Erdmann, R. Fast Fitting of Multi-exponential Decay Curves. *Opt. Commun.* **1997**, *134*, 371–378.
51. Antelman, J.; Wilking-Chang, C.; Weiss, S.; Michalet, X. Nanometer Distance Measurements between Multicolor Quantum Dots. *Nano Lett.* **2009**, *9*, 2199–2205.
52. Williams, R.; Labib, M. E. Zinc Sulfide Surface Chemistry: An Electrokinetic Study. *J. Colloid Interface Sci.* **1985**, *106*, 251–254.
53. Duran, J. D. G.; Guindo, M. C.; Delgado, A. V. Electrophoretic Properties of Colloidal Dispersions of Monodisperse Zinc Sulfide: Effects of Potential-Determining Ions and Surface Oxidation. *J. Colloid Interface Sci.* **1995**, *173*, 436–442.
54. Mizoguchi, T. Aqueous Oxidation of Zinc Sulphide, Pyrite and Their Mixtures in Hydrochloric Acid. *Trans. Inst. Min. Metall., Sect. C* **1983**, *92*, C14–C19.
55. Chirita, P.; Descostes, M.; Schlegel, M. L. Oxidation of FeS by Oxygen-Bearing Acidic Solutions. *J. Colloid Interface Sci.* **2008**, *321*, 84–95.
56. Young, E. M. Electron-Active Silicon Oxidation. *Appl. Phys. A: Mater. Sci. Process.* **1988**, *47*, 259–269.
57. Sharp, I. D.; Xu, Q.; Yuan, C. W.; Beeman, J. W.; Ager, J. W.; Chrzan, D. C.; Haller, E. E. Kinetics of Visible Light

Photo-Oxidation of Ge Nanocrystals: Theory and *In Situ* Measurement. *Appl. Phys. Lett.* **2007**, *90*, 163118.
58. Tang, J.; Marcus, R. A. Mechanisms of Fluorescence Blinking in Semiconductor Nanocrystal Quantum Dots. *J. Chem. Phys.* **2005**, *123*, 054704.
59. Tang, J.; Marcus, R. A. Diffusion-Controlled Electron Transfer Processes and Power-Law Statistics of Fluorescence Intermittency of Nanoparticles. *Phys. Rev. Lett.* **2005**, *95*, 107401.
60. Frantsuzov, P. A.; Marcus, R. A. Explanation of Quantum Dot Blinking without the Long-Lived Trap Hypothesis. *Phys. Rev. B* **2005**, *72*, 155321.
61. Rosen, S.; Schwartz, O.; Oron, D. Transient Fluorescence of the Off State in Blinking CdSe/CdS/ZnS Semiconductor Nanocrystals Is Not Governed by Auger Recombination. *Phys. Rev. Lett.* **2010**, *104*, 157404.
62. Wang, L.-W. Calculating the Influence of External Charges on the Photoluminescence of a CdSe Quantum Dot. *J. Phys. Chem. B* **2001**, *105*, 2360–2364.
63. Jha, P. P.; Guyot-Sionnest, P. Trion Decay in Colloidal Quantum Dots. *ACS Nano* **2009**, *3*, 1011–1015.
64. Fisher, B.; Caruge Jean, M.; Zehnder, D.; Bawendi, M. Room-Temperature Ordered Photon Emission from Multiexciton States in Single CdSe Core−Shell Nanocrystals. *Phys. Rev. Lett.* **2005**, *94*, 087403.
65. Zhao, J.; Nair, G.; Fisher, B. R.; Bawendi, M. G. Challenge to the Charging Model of Semiconductor-Nanocrystal Fluorescence Intermittency from Off-State Quantum Yields and Multiexciton Blinking. *Phys. Rev. Lett.* **2010**, *104*, 157403.
66. Gomez, D. E.; van Embden, J.; Mulvaney, P.; Fernee, M. J.; Rubinsztein-Dunlop, H. Exciton-Trion Transitions in Single CdSe−CdS Core−Shell Nanocrystals. *ACS Nano* **2009**, *3*, 2281–2287.
67. Spinicelli, P.; Buil, S.; X., Q.; Mahler, B.; Dubertret, B.; Hermier, J. P. Bright and Grey States in CdSe−CdS Nanocrystals Exhibiting Strongly Reduced Blinking. *Phys. Rev. Lett.* **2009**, *102*, 136801.
68. Knappenberger, K. L.; Wong, D. B.; Romanyuk, Y. E.; Leone, S. R. Excitation Wavelength Dependence of Fluorescence Intermittency in CdSe/ZnS Core/Shell Quantum Dots. *Nano Lett.* **2007**, *7*, 3869–3874.
69. Crouch, C. H.; Mohr, R.; Emmons, T.; Wang, S.; Drndic, M. Excitation Energy Dependence of Fluorescence Intermittency in CdSe/ZnS Core−Shell Nanocrystals. *J. Phys. Chem. C* **2009**, *113*, 12059–12066.
70. Park, S.-J.; Link, S.; Miller, W. L.; Gesquiere, A.; Barbara, P. F. Effect of Electric Field on the Photoluminescence Intensity of Single CdSe Nanocrystals. *Chem. Phys.* **2007**, *341*, 169–174.
71. Kobitski, A. Y.; Heyes, C. D.; Nienhaus, G. U. Total Internal Reflection Fluorescence Microscopy: A Powerful Tool to Study Single Quantum Dots. *Appl. Surf. Sci.* **2004**, *234*, 86–92.